Journal of Physical Science and Application 4 (3) (2014) 150-158

Upconversion Luminescence of Er^{3+} and Co-Doped Er^{3+}/Yb^{3+} Novel Transparent Oxyfluoride Glasses and Glass Ceramics: Spectral and Structural Properties

Arzumanyan Grigory[1], Vartic Victoria[1], Kuklin Alexander[1, 2], Soloviov Dmitry[1, 2], Rachkovskaya Galina[3], Zacharevich Galina[3], Trusova Ekaterina[3], Skoptsov Nikolay[4], Yumashev Konstantin[4]

1. Joint Institute for Nuclear Research (JINR), Dubna, Russia

2. Moscow Institute of Physics and Technology, State University (MIPT), Dolgoprudny, Russia

3. Belarusian State Technological University (BSTU), Minsk, Belarus

4. Belarusian National Technical University (BNTU), Minsk, Belarus

Received: December 20, 2013 / Accepted: January 25, 2014 / Published: March 15, 2014.

Abstract: Transparent oxyfluoride silicate precursor glasses and glass ceramics with the novel composition (1) SiO_2-PbO-PbF_2-Er_2O_3, (2) SiO_2-GeO_2-PbO-PbF_2-Er_2O_3 (3) SiO_2-Al_2O_3-Y_2O_3-Na_2O-NaF-LiF-Er_2O_3-YbF_3 doped with Er^{3+} and co-doped with Er^{3+}/Yb^{3+} ions were synthesized. X-ray diffraction analysis (XRD) and Er^{3+} absorption spectra revealed precipitation of PbF_2 nanocrystals dispersed in the glassy matrix. Under 980 nm laser excitation, intense green, red and near IR bands of upconversion luminescence (UCL) were recorded both before and after heat treatment. In the glass ceramics the upconversion intensity increased significantly. To our knowledge, for the first time the composition of the glass ceramics characterized by the small-angle neutron scattering (SANS) showed the cluster organization of PbF_2 nanocrystals.

Key words: Visible to near-infrared upconversion, rare-earth luminescence, oxyfluoride glass ceramics, small-angle neutron scattering.

1. Introduction

Development of high-techs claims production of stable, energy-conserving and eco-friendly equipment. One of such techniques in optics is based on the upconversion effect. The basic ideas on upconversion were generated more than 50 years ago in papers by Bloembergen and Auzel [1-3]. Later, for several decades this process, which is actually an anti-Stokes type of radiation, was widely studied by many authors and had several important applications among which are shortwave lasers, various opto-electronic devices, biophosphors, etc. [4-10]. To date the interest to the phenomenon of upconversion has received a new impulse due to the synthesis of modern matrix elements that contain various nanocomposites.

Upconversion is most effective in doping of optically inert matrices with lanthanide ions. Fluorides, bromides, chlorides, iodides and other materials are most often used as glass matrices with low-phonon energy environment. Such environment prevents non-radiative losses of energy in the excited states of lanthanide dopants. Oxyfluoride glasses and based on them nanoceramics, that combine benefits of low-phonon energy of fluorides, chemical durability and mechanical stability of oxides, and high optical quality of silicate glasses are of special interest [11-14].

In present work, three oxyfluoride glasses with different composition of matrices were chosen for

Corresponding author: Arzumanyan Grigory, assistant professor, research fields: laser physics, luminescence, nanotechnologies and biophysics. E-mail: arzuman@jinr.ru.

studies of UCL: two of them were doped with Er^{3+} ions only, and one sample was co-doped with the pair Er^{3+}/Yb^{3+}.

2. Experiments

2.1 Samples

Glass matrices doped with Er^{3+} and Yb^{3+} ions were synthesized on the basis of two oxifluoride glass-forming low-melting systems:

(1) SiO_2-PbO-PbF_2-Er_2O_3;

(2) SiO_2-GeO_2-PbO-PbF_2-Er_2O_3 and one hard-melting system;

(3) SiO_2-Al_2O_3-Y_2O_3-Na_2O-NaF-LiF-Er_2O_3 -YbF_3.

The synthesis of the low-melting glass matrices was performed at 950 °C for 30 min in an electric silit furnace, and the synthesis of the high-melting matrix was done at 1,450 °C for 1 h in a gaseous open-flame furnace in corundum crucibles of 25 mL capacity in the atmosphere. The glasses obtained were annealed to relieve inner stresses. Flat-parallel polished samples of 1-2 mm thick were produced from the annealed glasses. The samples (1) and (2) were doped with the content of 1 mol% of Er_2O_3 (4.4×10^{20} cm^{-3}), and the sample (3) was doped with 0.3 mol% of Er_2O_3 (1.48×10^{20} cm^{-3}) and 4.3 mol% of YbF_3 (9.84×10^{20} cm^{-3}).

Nanosize oxyfluoride glass ceramics doped with Er^{3+} ions (samples 1 and 2) have been obtained on heat treatment of their precursor glasses at the glass transition temperature T_g. Heat treatment was performed at 350 °C from 5 to 40 h. The composition of the crystalline phase of PbF_2 was characterized by XRD results performed at the diffractometer D8 Advance, Bruker, according to the American X-ray card-index [15].

2.2 Setups

The upconversion luminescence was studied at the multimodal optical platform "CARS" (Fig. 1).

This platform has been developed for research in microscopy and spectroscopy of spontaneous Raman scattering and its nonlinear modification known as Coherent Anti-Stokes Raman Scattering (CARS). A detailed description of the platform can be found elsewhere [16, 17]. We used the opportunity to register the medium response to the IR laser excitation in the anti-Stokes region of the spectrum for UCL studies. Excitation was provided by a continuously tunable between 690-990 nm laser delivering 6 ps pulses at a repetition rate of 85 MHz and high spectral resolution of 3-5 cm^{-1} in the whole tuning range (model EKSPLA PT257-SOPO, Lithuania). The laser beam was focused into the sample by means of a 40× microscope objective lens with a numerical aperture of 0.6. The UCL spectra was analyzed with the monochromator-spectrograph MS-5004i and CCD camera.

2.3 Small Angle Neutron Scattering (SANS) Spectrometer YuMO

Small angle neutron scattering is a method of structural analysis of condensed matter with low space resolution by measurement and analysis of dependence of intensity of the coherent elastic scattered radiation on the scattering vector [18, 19]. The range of the values of the scattering vectors modules corresponds to the sizes of structural elements from fractions to hundreds of nanometers. The essential SANS feature is a non-destructive analysis of the inner structure of disordered systems. Its application is often the only way to obtain information about the structure of samples with chaotic

Fig. 1 Multimodal optical platform "CARS".

arrangement of inhomogeneities in the nano-size range [20].

SANS experiments were performed at the YuMO spectrometer (Fig. 2) of the IBR-2 pulsed reactor of the Joint Institute for Nuclear Research (JINR) [21, 22]. The diameter of the neutron beam can be varied from 8 to 22 mm with the intensity of up to 2.6×10^7 neutrons. The neutron flux scattered on the sample (8) comes into the vacuum neutron guide with ring detectors and direct beam detector. Monitoring and the control of the spectrometer parameters were carried out with the software SONIX [23]. Primary experimental data processing was done with the software package SAS [24, 25].

3. Results and Discussion

3.1 XRD and SANS Structural Investigations

X-ray diffraction analyses evidenced the lead fluoride PbF_2 nanocrystals precipitated in the glassy matrix of the (1) and (2) heat-treated samples. Fig. 3 shows the XRD curve of the glass ceramic: diffraction peaks exactly corresponds to the PbF_2 crystal lattice [14]. The diffraction patterns of the both heat-treated glasses (1) and (2) are identical.

The use of Scherrer equation enabled the mean size of PbF_2 nanocrystals to be evaluated about 9-10 nm in diameter.

The following mechanism of forming a nanocrystal phase of the lead fluoride in the glassy matrix can be expected: in the process of glass melting phase separation occurs in the melt. One of the phases is enriched with the lead fluoride. In the process of heat treatment, crystallization centers are generated on the border of phase separation; a crystal phase, the lead fluoride in this case, is formed and evolved around these centers with the growth of temperature and duration of the heat treatment. Trivalent ions of erbium embedded into the crystal lattice of the lead fluoride $PbF_2:Er^{3+}$.

The XRD data accord well with the SANS results. Fig. 4 shows normalized SANS curves of samples (1) and (2) before and after heat treatment (scattering in the sample absence was used as background).

The red curve corresponds to the glass ceramic, and the black curve to the precursor glass.

It can be definitely seen that the SANS curves for the precursor and the glass ceramic differ that indicates structural changes in glassy matrix after the heat-treating. In order to construct 3D model (ab initio model) of the nanocrystalline structure shape we used the software package ATSAS [26] and the SANS curves for the glass ceramic samples where their precursors were used as the background (Fig. 5). It leads to eliminate scattering both from the matrix itself and a non-coherent component as well.

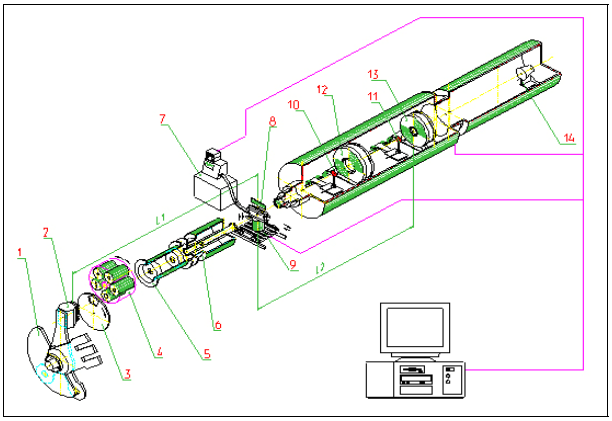

Fig. 2 Layout of the YuMO spectrometer。

(1) two reflectors; (2) moderator zone of the reactor; (3) chopper; (4) and (6) the first and the second collimators; (5) vacuum tube; (7) thermostat; (8) thermostat cassette with samples; (9) samples' table; (10, 11) Vn standards; (12) first ring-wire detector; (13) second ring detector, (14) direct beam detector.

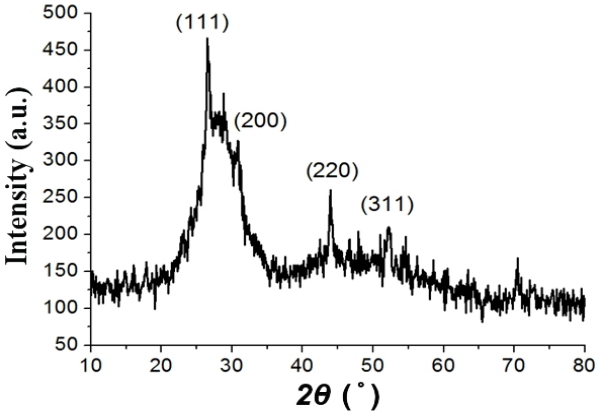

Fig. 3 The XRD curve of glass ceramic, Sample 1.

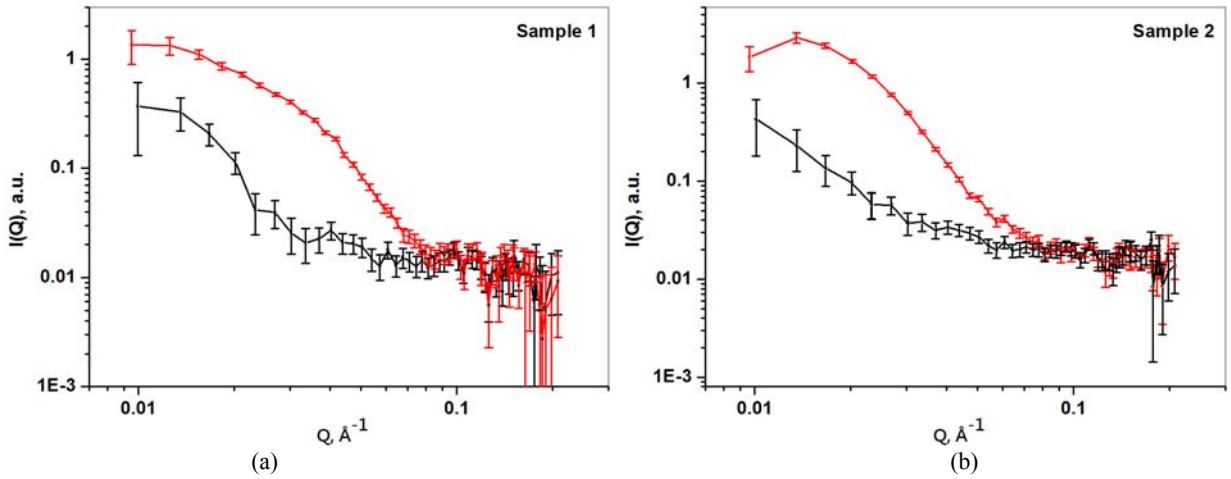

(a) (b)

Fig. 4 SANS curves for (a) Sample 1 and (b) Sample 2.

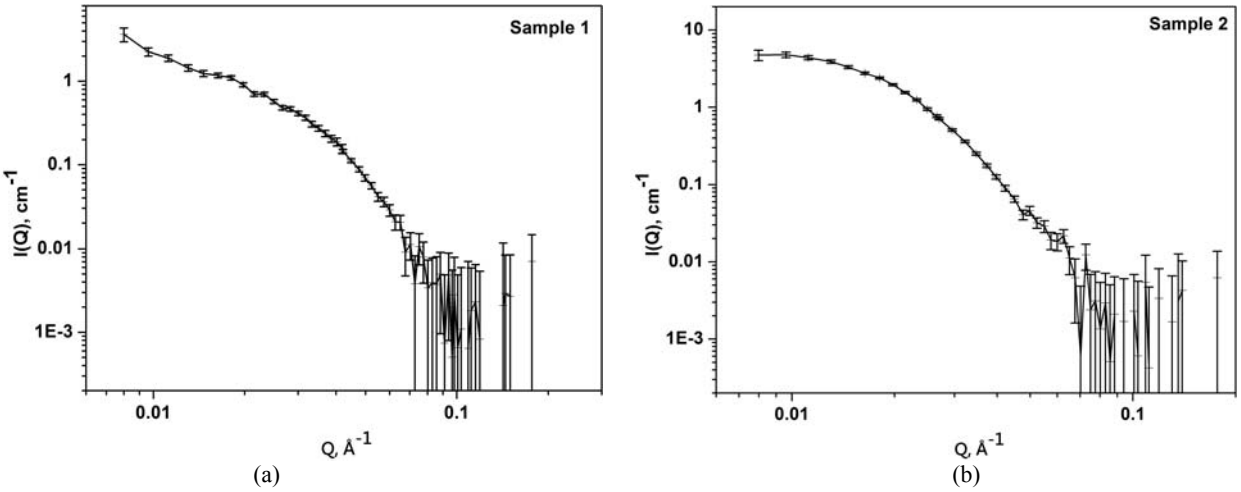

(a) (b)

Fig. 5 Differential cross section of scattering versus the value of the scattering vector module: (a) Sample 1 and (b) Sample 2.

Figs. 6 and 7 present the projection patterns of the obtained models of the PbF_2 nanocrystals shapes for Samples (1) and (2), respectively.

As a result of modeling, the sizes and shape of the nano-scaled structures of oxyfluoride glass ceramics evidenced to the cluster pattern organization of PbF_2 nanocrystals. The sizes for sample (1) are about 10 nm in cross section that coincides to the sizes of nanocrystals assessed by XRD, and 30 nm in the longitudinal direction. Proceeding from it we can presuppose that the clusters consist of 3-4 nanocrystals.

The PbF_2 cluster concentration in samples was calculated, assuming that neutron scattering occurs in PbF_2 clusters:

$$c = \frac{I_0}{(\Delta\rho)^2 \cdot V^2}$$

where, I_0 is the intensity in zero angle, $\Delta\rho$ is the difference of neutron scattering length densities of the matrix and PbF_2 clusters (contrast), V is the cluster volume.

The data are summarized in Table 1.

For the calculation we used the values of cluster volumes and scattering intensity at the zero angles that the ATSAS software package gives.

3.2 Absorption and Upconversion Luminescence Spectra

Absorption spectra were measured at the spectrophotometer Varian Cary 5000. Fig. 8 illustrates

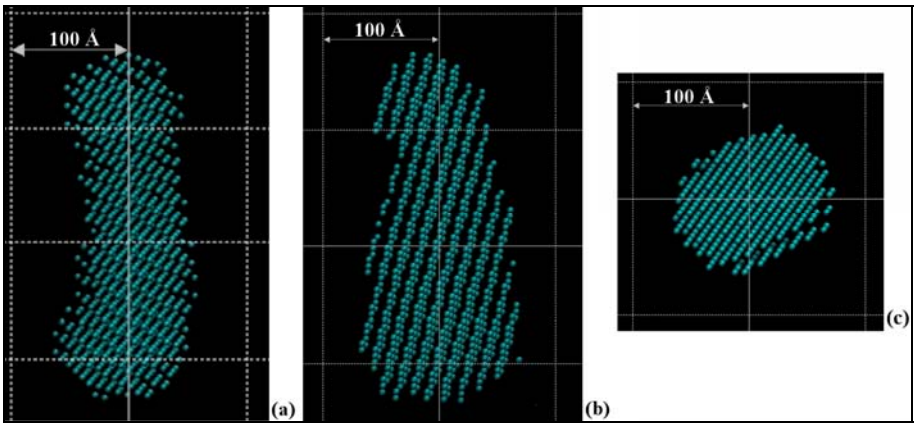

Fig. 6 Modeling results for sample (1): a, b, c, front, side and top views respectively.

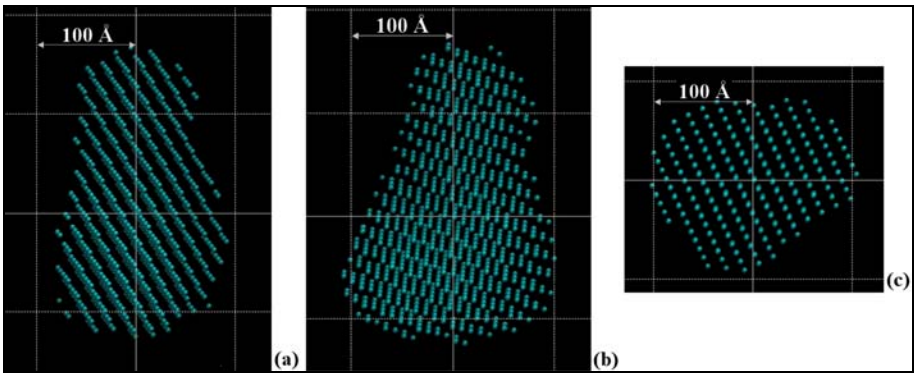

Fig. 7 Modeling results for sample (2): a, b, c – front, side and back views respectively.

Table 1 The calculated data for PbF_2 clusters, samples (1) and (2).

Sample	I_0 (cm^{-1})	$\Delta\rho$ ($Å^{-2}$)	V ($Å^3$)	c (cm^{-3})
(1)	2.2	4.29×10^{-6}	2.42×10^{6}	2×10^{14}
(2)	6.45	4.29×10^{-6}	4.94×10^{6}	1.4×10^{14}

the absorption spectra of Er^{3+} ions measured over the ranges of: (a) 500-570 nm, (b) 630-700 nm and (c) 780-820 nm. Three absorption bands were recorded in the visible part of the spectrum corresponding to the transitions: $^4I_{15/2} \rightarrow {}^2H_{11/2}$ (520 nm), $^4I_{15/2} \rightarrow {}^4S_{3/2}$ (540 nm) and $^4I_{15/2} \rightarrow {}^4F_{9/2}$ (650 nm). One more spectral band was recorded in the near IR range with the maximum centered around 800 nm that corresponds to the transition $^4I_{15/2} \rightarrow {}^4I_{9/2}$. For the Sample 2, the absorption curves are similar.

Due to changes of the co-ordination environment around the Er^{3+} ions in the glass ceramic samples the outer electron shells of Er^{3+} ions are distorted. This effect reveals itself in the absorption spectra curves: the Er^{3+} ions bands for glass ceramic become structured, and new peaks, which are more indicative for crystal matrices, appear.

Fig. 9c shows the absorption spectrum of Yb^{3+} ions (Sample 3); the transition $^2F_{7/2} \rightarrow {}^2F_{5/2}$ corresponds to it (peak at 976 nm). On the background of a strong absorption band of ytterbium, the Er^{3+} spectrum is vaguely distinguishable.

Fig. 10a presents the upconversion luminescence spectra of precursor samples under the excitation of a 980 nm laser beam. Fig. 10b shows the energy levels diagram of Er^{3+}/Yb^{3+} ions upon which the possible upconversion mechanisms is discussed.

Three dominant mechanisms are involved in the upconversion process: ground/excited state absorption (GSA/ESA), energy transfer (ET) and cross-relaxation (CR) [7, 8]. In the case of a glass matrix doped only with the Er^{3+} ions the metastable level $^4I_{11/2}$ is directly excited by 980 nm pump photon (GSA) and then further excited by a second photon to the level $^4F_{7/2}$ (ESA1). Besides, in the energy transfer process, two

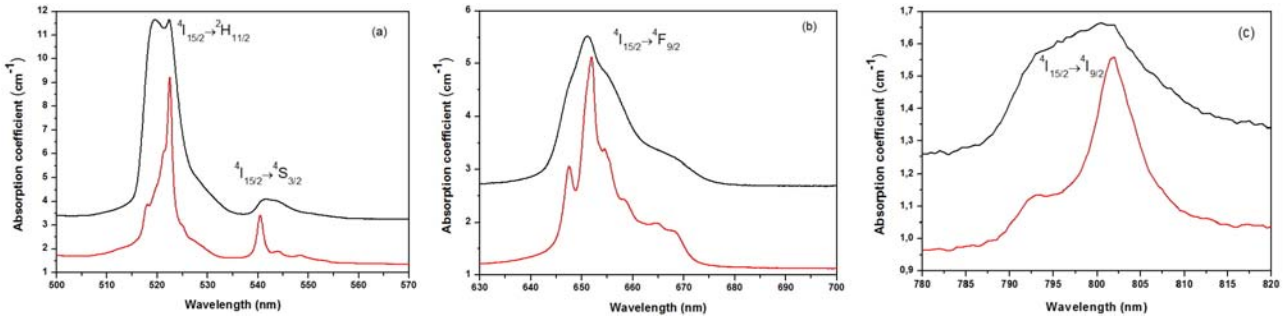

Fig. 8 Absorption spectra of sample (1) measured over the ranges of: (a) 500-570 nm, (b) 630-700 nm and (c) 780-820 nm. The black curve, precursor glass, the red curve, glass ceramics.

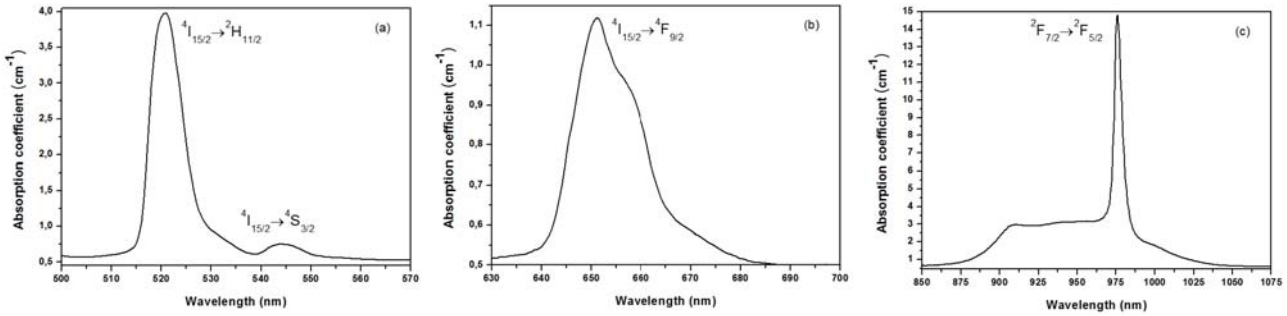

Fig. 9 Absorption spectra of sample (3) measured over the ranges of: (a) 500-570 nm, (b) 630-700 nm and (c) 850-1075 nm.

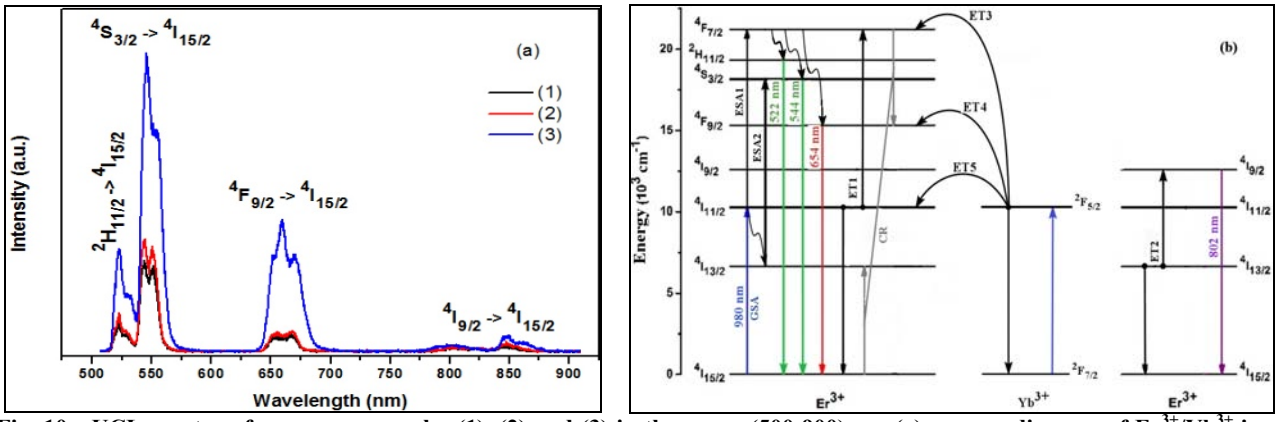

Fig. 10 UCL spectra of precursor samples (1), (2) and (3) in the range (500-900) nm (a), energy diagram of Er^{3+}/Yb^{3+} ions with possible mechanisms of UCL radiation (b).

excited Er^{3+} ($^4I_{11/2}$) ions interact with each other (ET1), thus also contribute to the population of the $^4F_{7/2}$ level. The UCL process can be accomplished by the non-radiative relaxations to the levels $^2H_{11/2}$, $^4S_{3/2}$, $^4F_{9/2}$ and further yield of three UC emissions ascribed to the transitions of $^2H_{11/2} \rightarrow {}^4I_{15/2}$ (522 nm), $^4S_{3/2} \rightarrow {}^4I_{15/2}$ (544 nm) and $^4F_{9/2} \rightarrow {}^4I_{15/2}$ (654 nm) respectively. The intensity ratio of green luminescence over red one is about 4 times. This can be assigned to the contribution of the ESA2 process to the population of $^4S_{3/2}$ level. We also recorded one more UCL band for the all precursor glasses in the near IR range with the peaks around 802 nm and 850 nm (Fig. 10a). We consider the ET2 process as responsible for this emission band.

As for the Sample (3) co-doped with Er^{3+}/Yb^3 ions it has already been clarified that the visible UCL emission under 970-980 nm excitation mainly result from resonant energy transfer between Yb^{3+} and Er^{3+} ions [e.g., 11 and references within]. The laser pump at about 980 nm occurs mostly into absorption band $^2F_{7/2} \rightarrow {}^2F_{5/2}$ of Yb^{3+} (Fig. 10b) as the absorption

cross-section of the Yb^{3+} band is several times stronger than $^4I_{15/2} \rightarrow {}^4I_{11/2}$ of Er^{3+} ions. Besides, the concentration of Yb^{3+} ions in Sample 3 is much larger than of Er^{3+} ions. It is evident that intensity of the UCL emission for this precursor sample is relatively stronger (blue curve in Fig. 10a).

Brief summary relative to precursor glasses: novel composition of transparent oxyfluoride precursor glasses studied for upconversion emission under 980 nm laser excitation showed sufficiently intense quantum yields of UCL in the visible and near IR range of spectra.

Finally, we present our impressive results on UCL spectra for glass ceramics. For a comparison, in Fig. 11 the UCL spectra are presented for silicate (Sample 1) and silico-germanate (Sample 2) oxifluoride glasses before and after their heat treatment at temperature 350 °C for 25 and 10 h, respectively. One can see that the emission intensities in glass ceramic increases: by factor of ~7 and ~40 in green and red bands respectively for the Sample 1, and significantly increases by factor of 25 (green) and ~150 (red) times for the Sample 2.

The UCL emission intensity rise in glass ceramics is due to the PbF_2 nanocrystals precipitated in the glassy matrix and can be characterized by the following factors: an interionic interactions of Er^{3+} ions which are mainly concentrated in the crystal lattice of PbF_2 followed by efficient near resonant cross-relaxation (CR) process [27]. This process with participation of the pair Er^{3+}-Er^{3+} ($^4F_{7/2}$, $^4I_{15/2} \rightarrow {}^4F_{9/2}$, $^4I_{13/2}$) is depicted in (Fig. 10b). As a result, the level $^4F_{9/2}$ is largely populated from level $^4F_{7/2}$ that leads to intensive red radiation. Secondly, by a much lower phonon energy of co-ordination environment around Er^{3+} ions in PbF_2 glass ceramic coupled to the phonon mode at ~250 cm^{-1} in comparison with that of precursor glasses (~1,000 cm^{-1}) [28]. Thus, the combination of above mentioned factors favor efficient upconversion emission of glass ceramic.

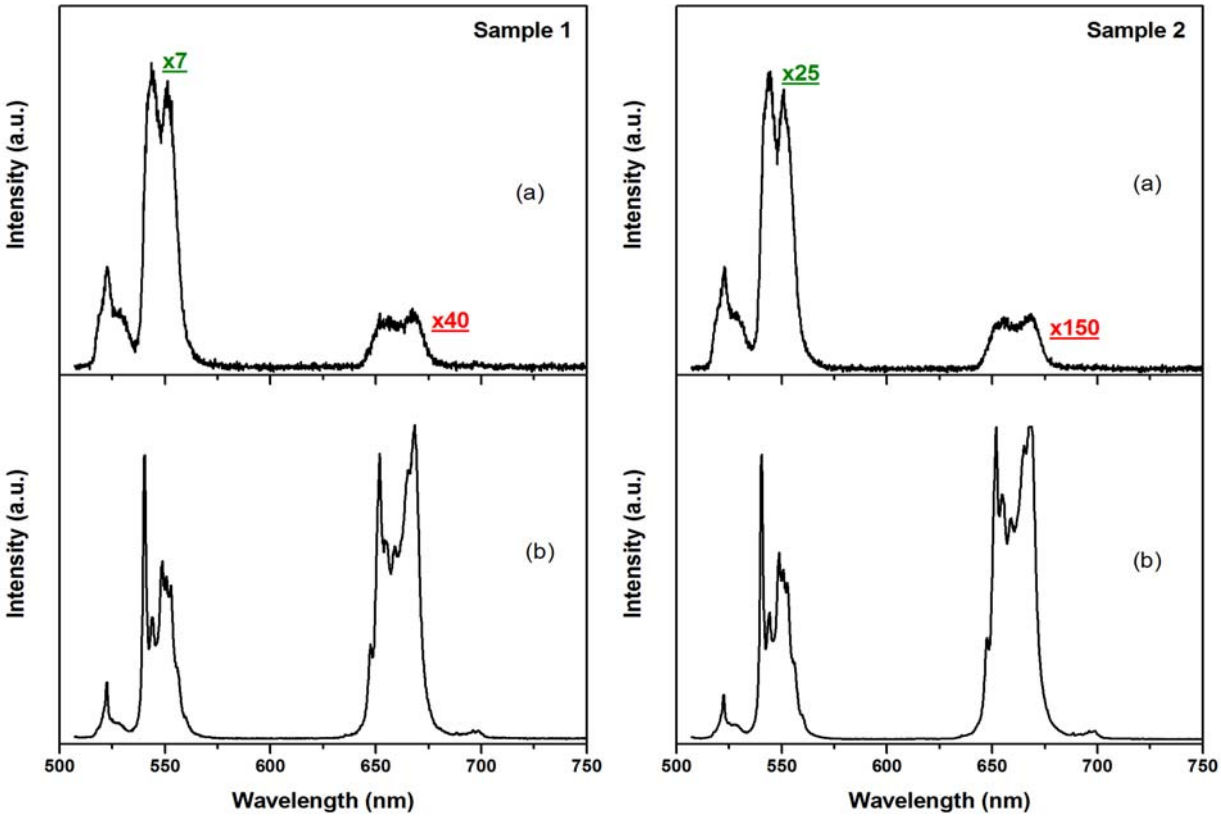

Fig. 11 UCL spectra of samples 1 and 2: (a) precursors and (b) glass ceramic.

4. Conclusions

We have developed a novel composition of transparent oxyfluoride silicate glasses and glass ceramics doped with Er^{3+} or Er^{3+}/Yb^{3+} ions. Precursor glasses display themselves sufficient intense upconversion emission in green, red and near IR ranges of spectra. Dramatic rise of UCL intensity by factor of ~ 150 was recorded for glass ceramic. To our knowledge, for the first time the structural features of glass ceramics characterized by the small-angle neutron scattering (SANS) showed the cluster organization of PbF_2 nanocrystals. Obtained results may be implemented for enhancement of quantum efficiency of various UC-based devices.

Acknowledgments

The authors express sincere gratitude to Dr. Anatoly Sharakovsky, senior researcher from the Institute of Solid State Physics, University of Latvia, for his fruitful comments and consultations.

References

[1] N. Bloembergen, Solid state infrared quantum counters, Phys. Rev. Lett. 2 (1959) 84.

[2] F. Auzel, Quantum counter by transfer of energy between two rare earth ions in mixture of tungstate and glass, C. R. Acad. Sci. (Paris) 262 (1966) 1016.

[3] F. Auzel, Quantum counter by energy transfer from Yb^{3+} to Tm^{3+} in a mixed tungstate and a germanate glass, C.R. Acad. Sci. (Paris) 263 (1966) 819-821.

[4] T. Trupke, A. Shalav, B.S. Richards, P. Wurfel, M.A. Green, Green efficiency enhancement of solar cells by luminescent up-conversion of sunlight, J. Sol. Energ. Mat. Sol. C. 90 (2006) 3327-3338.

[5] Y. Teng, J. Zhou, X. Liu, S. Ye, J. Qiu, Efficient broadband near-infrared quantum cutting for solar cells, J. Opt. Soc. Am. Opt. Express 18 (9) (2010) 9672.

[6] Y. Yang, Y.H. Zhang, W.Z. Shen, H.C. Liu, Semiconductor infrared up-conversion devices, Rev. J. Prog. Quantum Elec. 35 (2011) 77-108.

[7] D. Vennerberg, Z. Lin, Upconversion nanocrystals: synthesis, properties, assembly and applications, J. Sci. Adv. Mater. 3 (2011) 26-40.

[8] A. Shalav, B.S. Richards, M.A. Green, Luminescent layers for enhanced silicon solar cell performance: Up-conversion, J. Sol. Energ. Mat. Sol. C. 91 (2007) 829-842.

[9] S.K.W. MacDougall, A. Ivaturi, J. Marques-Hueso, K.W. Krämer, B.S. Richards, Ultra-high photoluminescent quantum yield of β-$NaYF_4$: 10% Er^{3+} via broadband excitation of upconversion for photovoltaic devices, J. Opt. Soc. Am. B 20 (S6) (2012) A879-A887.

[10] J. Chen, J.X. Zhao, Upconversion nanomaterials: synthesis, mechanism, and applications in sensing, IEEE Sens. J. 12 (2012) 2414-2435.

[11] Y. Wang, J. Ohwaki, New transparent vitroceramics codoped with Er^{3+} and Yb^{3+} for efficient frequency upconversion, Appl. Phys. Lett. 63 (24) (1993) 3268-3270.

[12] I. Gugov, M. Muller, C. Russel, Transparent oxyfluoride glass ceramics co-doped with Er^{3+} and Yb^{3+}-crystallization and upconversion spectroscopy, J. Solid State Chem. 184 (2011) 1001-1007.

[13] M.A.P. Silva, Synthesis and structural studies of Er^{3+} containing lead cadmium fluoroborate glasses and glass-ceramics, J. Braz. Chem. Soc. 13 (2002) 100-109.

[14] Powder Diffraction File, Inorganic Phases, JCPDS ICDD, 5 (1989) 592.

[15] L.I. Mirkin, Reference book on X-ray analysis of polycrystalline, USSR, 1961.

[16] G. Arzumanyan, Multimodal optical platform for Condensed matter studies, JINR Communication, P13-2013-47, Dubna, 2013.

[17] V. Kopachevsky, A. Kachinsky, A. Kuzmin, P. Prasad, G. Arzumanyan, S. Tyutyunnikov, Modern trends in nanoscience, Editura Academiei Romane, Bucureşti, 2013, pp. 11-28.

[18] L.A. Feigin, D.I. Svergun, Structure analysis by small-angle X-ray and neutron scattering, Plenum Press, New York, 1987.

[19] O. Glatter, A new method for the evaluation of small-angle scattering data, J. Appl. Crystallogr. 10 (5) (1977) 415-421.

[20] A.V. Belushkin, D.P. Kozlenko, A.V. Rogachev, Synchrotron and Neutron Scattering Methods for Studies of Properties of Condensed Matter: Complementarity or Competition?, JINR Preprint, P14 (2011) 18.

[21] A.I. Kuklin, A.K. Islamov, V.I. Gordeliy, Two-detector system for small-angle neutron scattering instrument, Neutron News 16 (2005) 16-18.

[22] A.I. Kuklin, A.Kh. Islamov, V.I. Gordeliy, Yu.S. Kovalev, P.K. Utrobin, Optimization two-detector system small-angle neutron spectrometer YuMO for nanoobject investigation, J. Surf. Investig.: X-ray, Synchrotron and Neutron Techniques 6 (2006) 74-83.

[23] A.S. Kirilov, E.I. Litvinenko, N.V. Astakhova, S.M. Murashkevich, T.B. Petukhova, V.E. Yudin, et al.,

Evolution of the SONIX software package for the YuMO spectrometer at the IBR-2 reactor, instruments and experimental techniques, Instrum. Exp. Tech. 47 (6) (2004) 334-336.

[24] A.G. Soloviev, E.I. Litvinenko, G.A. Ososkov, A.Kh. Islamov, A.I. Kuklin, Application of wavelet analysis to data treatment for small-angle neutron scattering, Nucl. Instrum. Methods Phys. Res. Sect. A 502 (2-3) (2003) 500-502.

[25] A.G. Soloviev, A.V. Stadnik, A.H. Islamov, A.I. Kuklin, The Package for Small-Angle Neutron Scattering Data Treatment, JINR Communication P10-2003-86, Dubna 2003.

[26] Data Analysis Software ATSAS 2.3, http://www.embl-hamburg.de/biosaxs/software.html.

[27] D. Chen, Y. Wang, Y. Yu, E. Ma, F. Bao, Z. Hu, et al, Influences of Er^{3+} content on structure and upconversion emission of oxyfluoride glass ceramics containing CaF_2 nanocrystals, Mater. Chem. Phys. 95 (2006) 264-269.

[28] Y. Kawamoto, R. Kanno, J. Qiu, Upconversion luminescence of Er^{3+} in transparent SiO_2-PbF_2-ErF_3 glass ceramics, J. Mater. Sci. 33 (1998) 63-67.